Influence of co-milling oxide physical properties on the structural changes of natural clinoptilolite zeolites

Narantsogt Natsagdorj[1], Narangarav Lkhagvasuren[1], Bolortuya Munkhjargal[1] and Jadambaa Temuujin[2]*

[1] School of Mathematics and Natural Sciences, Mongolian National University of Education, 14191, Ulaanbaatar, Mongolia

[2] CITI University, Denver Street, 14190, Ulaanbaatar, Mongolia

**Author to whom correspondence should be addressed*

Jadambaa Temuujin

CITI University

Denver Street, 14190 Ulaanbaatar, Mongolia

E-mail: temuujin.jadamba@citi.edu.mn
ORCID: https://orcid.org/0000-0003-0930-7271

Please cite this article as: Narantsogt N., Narangarav L., Bolortuya M, and Jadambaa T. Influence of co-milling oxide physical properties on the structural changes of natural clinoptilolite zeolites. *Mongolian Journal of Chemistry*, **24**(50), 2023, xx-xx
https://doi.org/10.5564/mjc.v24i50.1250

Influence of co-milling oxide physical properties on the structural changes of natural clinoptilolite zeolites

Narantsogt Natsagdorj[1], https://orcid.org/0000-0002-1040-1276
Narangarav Lkhagvasuren[1],
Bolortuya Munkhjargal[1],
Jadambaa Temuujin[2*], https://orcid.org/0000-0003-0930-7271

[1] *School of Mathematics and Natural Science, Mongolian National University of Education, 210648 Ulaanbaatar, Mongolia*
[2] *CITI University, Denver Street, 14190, Ulaanbaatar, Mongolia*

ABSTRACT

Zeolites are a family of open-framework aluminosilicate minerals used in many diverse fields, including building materials, agriculture, water treatment, and catalysis.

In this study, natural zeolites were mechano-chemically treated by co-milling with corundum and cristobalite. The idea behind the study was that co-milling with high-hardness oxides would cause natural zeolite to undergo more structural distortion, potentially increasing its reactivity and sorption capabilities. Corundum has a density of 3.95 g/cm^3 and a hardness of 9, while cristobalite has a density of 2.27 g/cm^3 and a hardness of 6-7, according to the Mohs hardness scale.

In a planetary ball mill, the zeolites and 20 wt.% of various oxides were co-ground for 30 min. The grinding media used were hardened steel balls with a weight ratio of 20:1 between the balls and the minerals. Raw minerals and milled products were evaluated using X-ray diffraction, Fourier-transform infrared spectroscopy and scanning electron microscopy.

It revealed that co-milling with different hardness oxides had a minor effect on the structural distortion of raw zeolite. Crystallite size reduction and amorphization were observed in high-hardness oxides rather than in zeolite particles. After milling, the amorphization of natural zeolite milled alone was 30.4%, while no significant amorphization was observed when co-milled with corundum and cristobalite. Preliminary results of Cr(VI) adsorption tests on raw and milled zeolites indicate that co-milling with high-hardness oxides is not the preferred method to enhance the activity of natural zeolite.

Keywords: Natural zeolite, co-milling, mechano-chemical treatment, corundum, cristobalite, FTIR, XRD, adsorption, Cr(VI)

INTRODUCTION

Natural zeolites are microporous aluminosilicate minerals that have many uses in industry, agriculture, medicine, and the environment. They are formed when volcanic rocks and alkaline groundwater interact. Natural zeolites are crystals that grow in the voids of sedimentary rocks or basalt rocks that arise under various geological conditions [1, 2]. Natural zeolites have received interest since the 1850s due to their base-exchange capabilities, which can be used in water softeners and agricultural applications [1, 3]. Zeolites are used today primarily as wastewater and gas pollution removers, catalysts, pesticides, and fertilizer carriers in food and agriculture, soil supplements, and animal feed additions [1, 2, 4]. Due to the contamination of industrial wastewater discharges, which contain many toxic heavy metals such as cadmium, chromium, lead, and mercury, the levels of toxic heavy metals in surface and ground waters have been rising recently [5].

Chromium is regarded as a high-priority environmental pollutant among hazardous heavy metals. The most prevalent chromium compounds have an oxidation state of (III) or (VI) and are considered hazardous to the environment [6]. Because of its solubility in practically the whole pH range, greater mobility than Cr(III), and chromium's carcinogenic state, Cr(VI) is more dangerous than Cr(III). Cr(III) is less poisonous and less mobile than Cr(VI) [6].

Although natural zeolites are used for many different things, their use is restricted because of their low purity and small channel diameter, which precludes the adsorption of larger gas molecules and organic compounds. Zeolites can be activated using a variety of techniques, such as mechanochemical activation, to improve their inherent qualities. The production of amorphous powders from elemental metals or powder mixes by ball milling, also known as mechanical grinding (MG), has been shown to be an effective way of optimizing the properties of the powder [7-9]. Mechanical activation of natural zeolite leads to amorphous products with a higher surface area and adsorption properties than raw zeolite [8, 9]. Previous references [10, 11] provide contradictory results in the sorption research of mechanically milled clinoptilolite. The mechanically amorphized clinoptilolite's cation exchange capacity (CEC) increased, according to Zolzaya *et al*. [10]. In contrast, Bohacs *et al*. discovered that methylene blue adsorption is maintained in mechanically activated clinoptilolite [11]. Mechanical amorphization can be accomplished by milling the crystalline compounds alone or in conjunction with other crystalline compounds; however, in the latter case, the mechanochemical production of a new amorphous or crystalline compound is also possible. Amorphization of the crystalline co-milling compounds is expected to rise if one of the compounds has a higher hardness than another. It was thought that the co-milled oxides' high hardness might also serve as a milling medium, accelerating the amorphization of the softer co-milling compound. Therefore, a study of the structures of

mechanically activated zeolite with the different oxides could clarify the influence of the hardness of the co-milled oxide on the sorption properties of the milled samples. This study aims to clarify how co-milling oxide hardness affects the amorphization and adsorption characteristics of natural zeolite. In this study, X-ray diffraction (XRD), Fourier transform infrared (FTIR), and scanning electron microscopy (SEM) were used to analyze the mechanochemical effects on natural zeolites caused by co-milling with different hardness oxides using a planetary ball mill. The impact of co-milling natural zeolites with different hardness oxides on the reactivity of the original zeolite was checked using Cr (VI) adsorption tests.

EXPERIMENTAL

Materials: Natural zeolite was obtained from the Tsagaan tsav deposit in southern Mongolia. The zeolites were dried at room temperature before being pulverized by hand to reduce particle size with a ceramic pestle and mortar.

Mechanically activated zeolite preparation: Corundum and cristobalite oxides were added to the zeolite for co-milling. Corundum has a density of 3.95 g/cm^3 and a Mohs hardness of 9. Cristobalite has a density of 2.27 g/cm^3 and a Mohs hardness of 6. Cristobalite was created by calcinating quartz oxide for 4 hours at 1300 ° C. Quartz was converted to Cristobalite to decrease the hardness for a better comparison with Corundum and to show the influence of hardness on the amorphization of natural zeolite. Some raw zeolites were ground alone and used as a reference.

A planetary ball mill (NQM-0.4, China) was used to grind raw or mixed zeolites. Natural zeolite 80% w/w + oxides 20% w/w make up co-milled zeolite samples. The grinding was carried out in a hardened steel pot with a volume of 121 cm^3. The ball-to-powder weight ratio was 20:1 and the grinding media was hardened steel balls with diameters of 0.6 cm. The samples (5.5 g) were milled at 1500 rpm at room temperature for 30 minutes.

Characterization: Chemical analysis (XRF): Chemical analyzes of the zeolite samples were performed by XRF (Shimadzu, Primini-X-ray fluorescence, Japan) using the pressed tablet.

SEM analysis: Scanning electron microscope (SEM) TM 1000 (Hitachi, Japan) was used to study the surface morphology of the raw and activated zeolites. Before the analysis, the aluminum stubs were coated with an adhesive. The samples were strewn across the stubs. To prevent static charge, the samples were gold coated with an Emscope SC500 Sputter coater.

XRD analysis: Mineralogical characterization was performed using powder XRD instruments (Shimadzu, MAXima-X XRD-7000, Japan). Measurements were carried out with Cu Kα radiation wavelength of 1.54056 Å, angle of 2 θ (5-60°) and scanning step size of 0.02°. After milling to determine the degree of amorphization, the following equation was used:

$$A = 100 - K, \%; \qquad K = \frac{I_{act}}{I_{raw}} \cdot 100, \% \tag{1}$$

-amorphization%, - crystallinity%, I_{act}-X-ray diffraction intensity of activated sample, I_{raw}-X-ray diffraction intensity of the raw sample. For the calculation of the amorphization rate, the average of the (*020*) and (*131*) peaks was used.

For approximate crystallite size determination was used Scherrer equation:

$$D = \frac{K\,\lambda}{\beta\,cos\theta} \tag{2}$$

D - mean size of crystallites, K – shape factor constant roughly 0.90, depends on the shape of crystallites, β - full width at half maximum in radians, λ - X-ray wavelength,

The non-overlapping (*020, 131, 151)* peaks were used to determine the crystallite size of the zeolite. For the cristobalite (*111, 102, 200)* peaks and for corundum (*012, 104, 113)* peaks were used.

FTIR analysis: The Shimadzu, Fourier transform infrared spectrometer (FTIR 8200PC, Japan), was used for the measurements by using 100 scans at 4 cm^{-1} resolutions, over the IR region of 400–4000 cm^{-1}. An air background spectrum was collected at the start of the sample analysis. Samples were diluted with spectroscopic purity KBr at powder weight ratio to KBr 1:200. The zeolite samples were measured three times and averaged for further processing. A background spectrum was measured before every sample to compensate for atmospheric conditions around the FT-IR instrument.

Adsorption test of Cr(VI): Only to determine whether the reactivity of the zeolites milled alone and in combination with other materials changed, a sorption test was conducted. A batch adsorption experiment was performed to determine the effectiveness of removing Cr(VI). According to a review of the literature, acidic media are preferred for the adsorption of Cr(VI). To conduct the adsorption test, we utilized pH 2. The pH variation and adsorption terms were not explored because the adsorption was not the main objective of the investigation. At 23°C +/- 2°C, batch studies were carried out in beakers at a batch rate of 0.5 g of zeolite per 50 mL of fluid. In glass beakers containing 50 mL of chromium standards, raw zeolite (clinoptilolite), milled zeolite, zeolite milled with corundum, and zeolite milled with cristobalite were added, respectively.

All the reagents used were analytical grade. The 1000 mg/L chromium standards were prepared from $K_2Cr_2O_7$ (Sigma). After 30 minutes of reaction time, the sorbents were removed by filtration through a laboratory filter paper for qualitative analysis and the residual concentration of chromate ions was determined by the UV-Vis spectrophotometric method.

The samples were tested for adsorption of Cr (VI) and its removal %.

$$Q_e = \frac{(C_i - C_e)}{w} * \mathrm{V} \quad (3)$$

$$Cr\ (VI)\ removal\ \% = \frac{(C_i - C_e)}{C_i} * 100 \quad (4)$$

Where Q_e is amount of adsorbed Cr(VI), C_i and C_e are the initial and equilibrium Cr(VI) concentrations of the test solution (mg/L), V is the test solution at volume (L), and W is the amount of adsorbent (g).

Batch experiments were performed in duplicate and the average value was used.

RESULTS AND DISCUSSION

Characterization of zeolite: Table 1 shows the results of the chemical analysis of natural zeolite. According to Table 1, the main elements of natural zeolite are SiO_2, Al_2O_3, K_2O, Na_2O, and Fe_2O_3.

Clinoptilolite is the primary crystalline phase of raw zeolite, according to the XRD pattern (Fig. 2A) of the material. The Si to Al molar ratio is 5.44. K^+>Na^+>Ca^{2+}>Mg^{2+} are the primary exchangeable cations. Illite and feldspar are examples of aluminosilicate minerals that may also be present based on chemical analysis.

Table 1. Chemical composition of natural zeolite, weight%

SiO_2	Al_2O_3	K_2O	Na_2O	Fe_2O_3	CaO	Cl	MgO	TiO_2	SrO	P_2O_5	MnO	SO_3
72.6	14.8	4.2	3.54	2.16	1.51	0.0307	0.709	0.207	0.125	0.042	0.0094	0.066

SEM micrographs (Fig. 1) show that natural zeolite consists of particles with the main sizes of 50 to 300 μm. The raw corundum represents chunky particles with varying sizes of 50-400 μm, while the cristobalite represents spherical morphology particles with sizes of ≈50 μm.

The particle sizes of the samples were substantially smaller after grinding. Particles smaller than 100 μm in size make up the milled samples. The larger particles with diameters of 100 μm should represent oxide particles, whereas the smaller particles should represent natural zeolites, because natural zeolites are considerably softer than oxide particles. This assertion might be supported by the fact that the milled zeolite contains smaller particles than those that were milled along with the oxide particles.

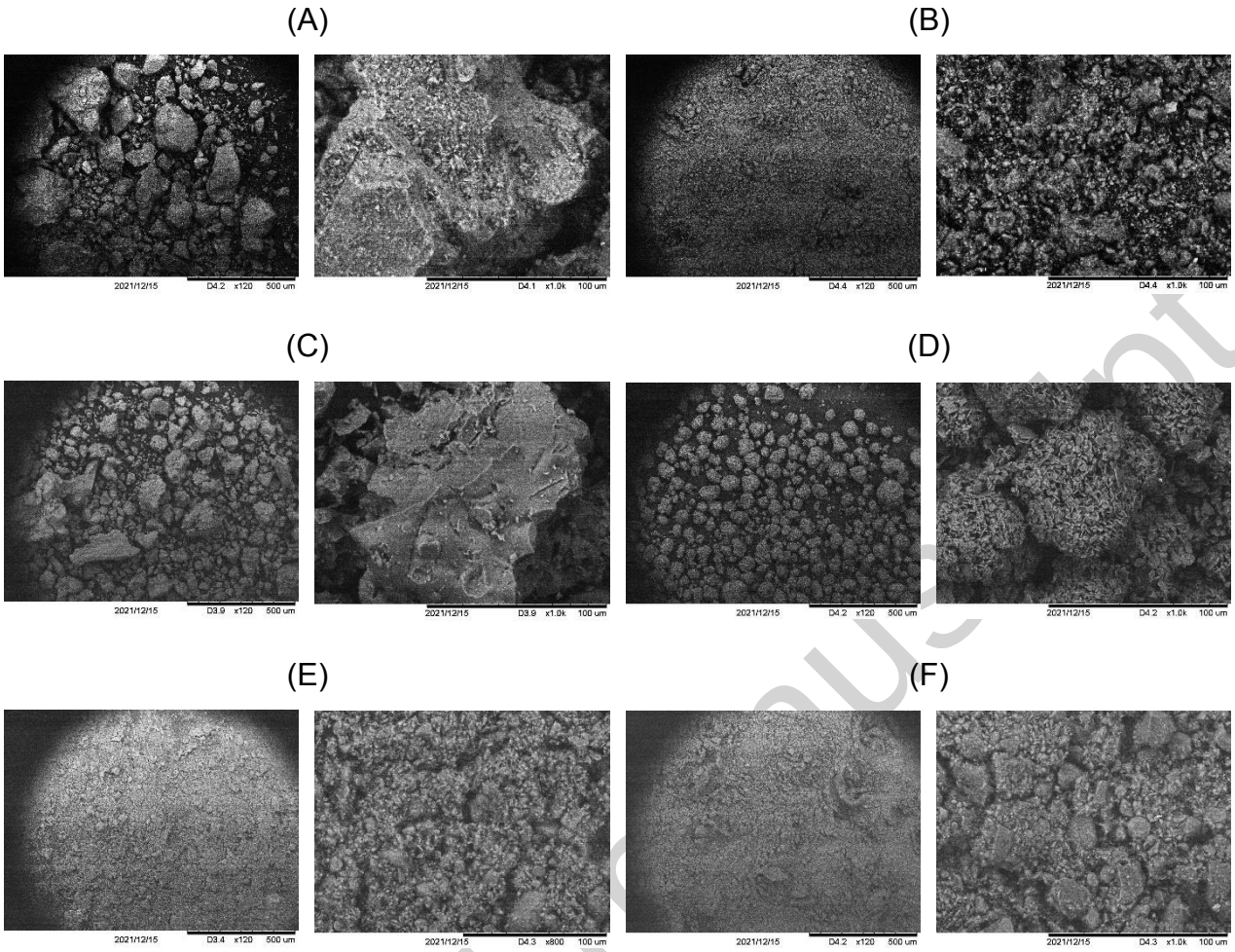

Fig. 1. SEM images of raw zeolite (A), activated zeolite (B), raw corundum (C), raw cristobalite (D), zeolite activated (co-milled) with corundum (E) and zeolite activated with cristobalite (F) at different magnification.

The XRD patterns of raw, milled, and co-milled with oxides zeolite samples are shown in Fig. 2. Clinoptilolite is the primary crystalline phase in raw samples, with illite and feldspar as minor impurities. The composition of Tsagaan tsav natural zeolite is similar to that of natural zeolites from deposits in Slovakia and Ukraine [12].

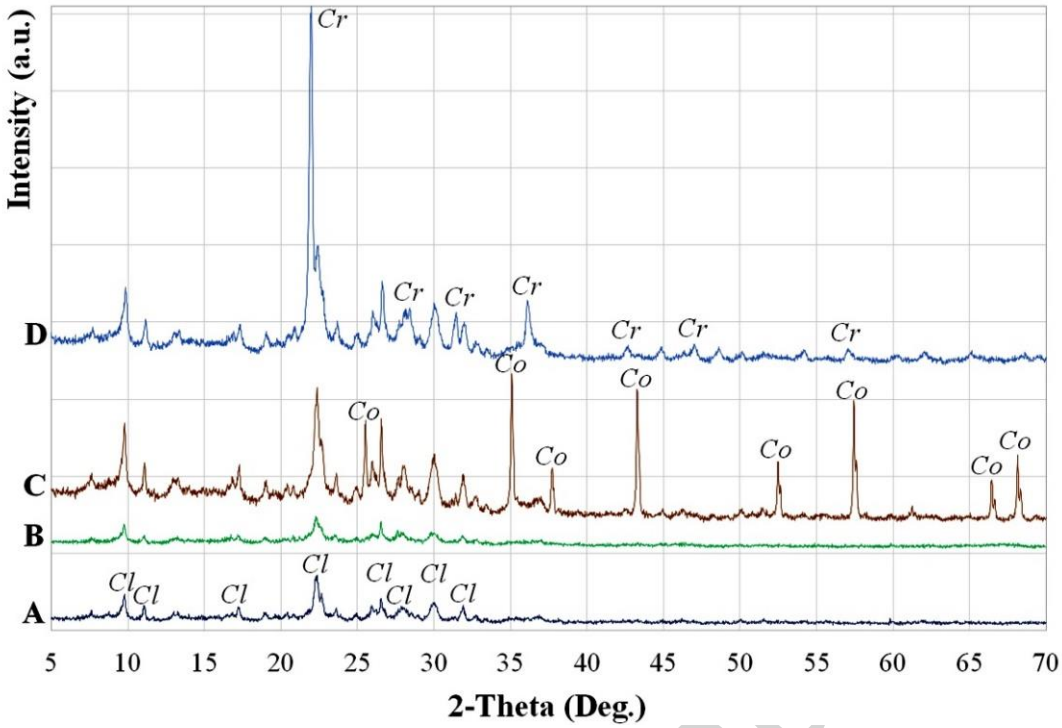

Fig. 2. XRD pattern of zeolite (A-raw zeolite/clinoptilolite; B-milled zeolite; C- zeolite co-milled with corundum; D- zeolite co-milled with cristobalite), (*Cl* – Clinoptilolite; *Co* – Corundum; *Cr* – Cristobalite)

Grinding of natural zeolite alters the structure of zeolite and lowers XRD intensity (Fig.2B). Formula (1) determined that the amorphization rate of clinoptilolite milled alone was approximately 30.4%. However, there are many overlapped peaks, making it difficult to accurately characterize them. However, almost no amorphization of clinoptilolite was observed in the co-milled corundum and cristobalite oxide particles. Milling, in general, reduces crystallite size while increasing strain to a particular limit of crystallite and strain. Then, as the milling time increases, the crystallite size is usually observed to increase as a result of agglomeration of the milled particles. It can be argued that the soft natural zeolite particles are agglomerating, consequently their crystallite size change is insignificant.

The estimated crystallite size of the raw zeolite, the raw oxides and the co-milled oxide and zeolite samples determined by formula (2) is shown in Table 2. The crystallite size of the milled zeolite was dramatically reduced from 22.58 to 15.84 nm. However, the crystallite sizes of the zeolites in co-milled samples were almost identical to those of the raw zeolites. The average crystallite size of zeolite co-milled with corundum was 22.63 nm and 18.02 nm with cristobalite. In other words, virtually little mechanically induced zeolite amorphization occurred during milling. The amorphization of the oxide particles happens easier than that of the clinoptilolite particles, according to XRD patterns of the co-milled oxides zeolite samples. In other words, the structural integrity of the soft zeolite did not change significantly when it was co-milled with the high

hardness oxides. Hard oxide particles experience preferential amorphization and a reduction in crystallite structure. Unexpected data showed that our first hypothesis was wrong.

Table 2. Approximate crystallite size of the raw and milled samples determined by Scherrer equation

Samples	The Miller indices (hkl)	Average D (nm)
Raw zeolite	020	22.58
	131	
	151	
Milled zeolite	020	15.94
	131	
	151	
Raw corundum	012	52.20
	104	
	113	
Crystallite size of the corundum milled with zeolite	012	46.94
	104	
	113	
Raw cristobalite	111	29.73
	102	
	200	
Crystallite size of the cristobalite milled with zeolite	111	22.67
	102	
	200	

Due to its extreme hardness, corundum is the mineral that is frequently used as an abrasive. The following are the used milling media and powders hardness: clinoptilolite < cristobalite < hardened steel < corundum. The following are the densities of the same materials: zeolite < cristobalite < corundum <hardened steel. The current study reveals that the density of the milling media possibly has a greater impact on the microstructure of the milled powders than the hardness of the powders being employed.

The total alkali-silica (TAS) diagram, which is based on the total alkali (K_2O+Na_2O) and silica (SiO_2) ratio of volcanic rocks, indicates (not shown here) that the used zeolite is found in the rhyolite area or is the same as the Idaho zeolite deposit of the tuff enriched in SiO_2 [12]. According to one theory, clinoptilolite typically develops from tuffs as a devitrified byproduct of volcanic glass or appears in rhyolite holes [13]. The TAS diagram supports this assertion.

In Fig. 3, the mid-FTIR spectra of raw, milled, and co-milled zeolite with corundum and cristobalite are shown in the lattice vibrations (4000-400 cm^{-1}) area.

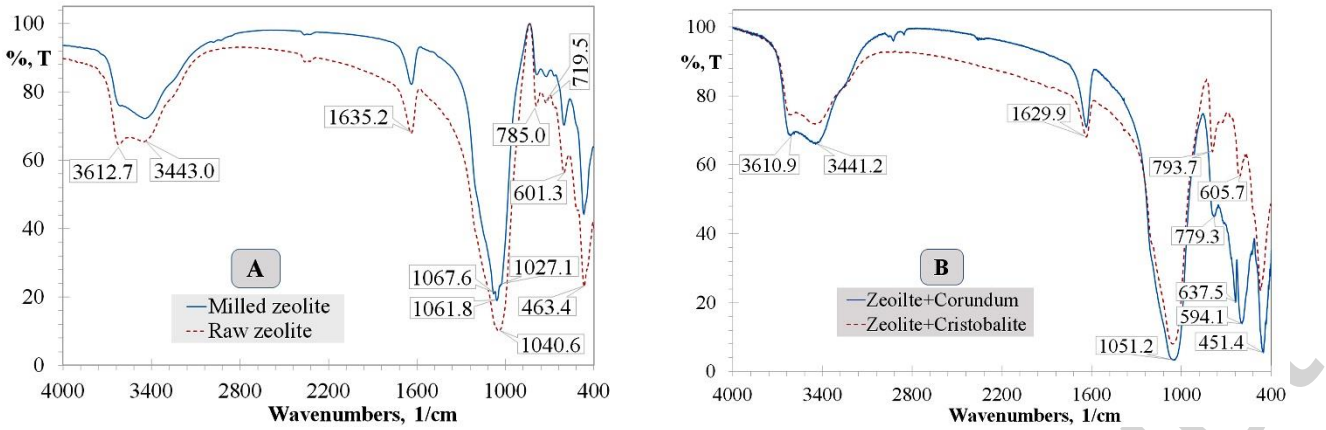

Fig. 3. FTIR spectrum of raw zeolite and milled zeolite (A) and zeolite milled with corundum and cristobalite (B).

The primary adsorption bands in raw clinoptilolite are located at 463, 601, 719, 785, 1041, 1635, 3443, and 3612 cm^{-1}. The raw clinoptilolite FTIR spectra closely resemble those provided by Bohacs *et al*., Putra and Kusumawati, and Mansouri *et al*. [11, 14, 15]. At 1040 cm^{-1}, a large broadband was seen. At 1635, 3443, and 3612 cm^{-1}, the bands are present. The hydroxyl of illite [11], silanol, or aluminol (Si-O(H)-Al bridging hydroxyls) groups associated to Broensted acidity [14] are assigned to the band over 3600 cm^{-1}. The water molecules linked to the native zeolite structure are responsible for the bands at 3443 and 1635 cm^{-1} [11, 15]. Near 1040, 785, and 463 cm^{-1}, additional bands can be seen. The 1040 cm^{-1} band corresponds to asymmetric stretching vibration modes of internal T–O bonds in TO_4 tetrahedra (T = Si and Al) as previous authors have always described [11, 15]. The 785 and 463 cm^{-1} bands are assigned to the stretching vibration modes of O–T–O groups and the bending vibrations of T–O bonds [16].

Some authors [11] described the appearance of the shoulder at wave number 860-920 cm^{-1} as a result of mechanically induced crystallite size decrease in the zeolite and a broadening band at 1060 cm^{-1} as a result of mechanical amorphization. Such alterations in the FTIR spectrum were not observed in the current study of mechanically milled clinoptilolite. The zeolites co-milled with the corundum and cristobalite (Fig. 3B) displays distinct bands for the zeolites, the typical band of the corundum at 590 and 637 cm^{-1}, and the cristobalite at 793 cm^{-1} [17, 18]. The water band centered at 1630, 3441, and 3661 cm^{-1} grew more in the zeolite sample co-milled with corundum than in the co-milled cristobalite sample. It implies that zeolite and corundum mixes adsorb more water than zeolite and cristobalite blends. As a result, higher porosity and amorphization of zeolite in the co-milled with corundum than in the co-milled with cristobalite, which in agreement with the crystallite size data provided in Table 2.

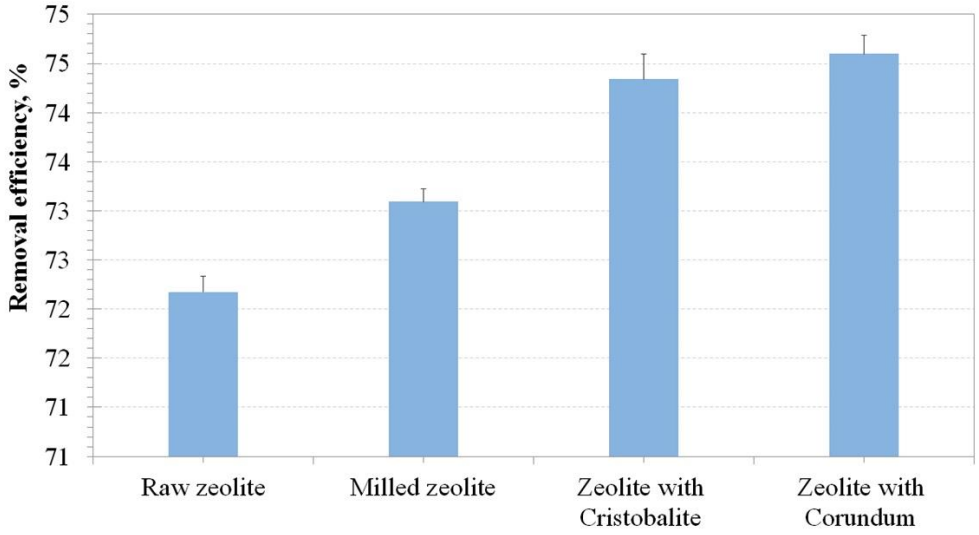

Fig. 4. Removal efficiency (%) of Chromium (VI) adsorption by raw zeolite and milled zeolite with corundum and cristobalite.

Fig. 4 demonstrates that the Cr(VI) removal effectiveness of milled samples (eq. 4) is relatively similar each other. Because the sorption test was not performed under optimal conditions, the presented results should be interpreted as the comparative value of each sample under the conditions described in the Characterization section. The removal efficiency of zeolites co-milled cristobalite and corundum is comparable to that of milled zeolite sample. Minimal changes in removal efficiency may indicate that structural changes in zeolite were not favorable in the mechanically milled zeolite's cation exchange capacity, confirming previous research [11]. The results of a preliminary study on the Cr(VI) adsorption of raw, milled and co-milled with corundum and cristobalite zeolites show that co-milling with high hardness oxides is not the best method for enhancing the reactivity of natural zeolite in terms of adsorption effectiveness. In comparison to zeolite milled alone, agglomeration and microstructural changes in soft and low-density natural zeolites that are co-milled with high hardness oxides are minimal. As shown by the Cr(VI) adsorption test, the reactivity of the co-milled natural zeolite was not improved. Co-milling oxides should have a higher density than high hardness if the natural zeolite is required to undergo greater structural changes.

CONCLUSIONS

Natural zeolites milled alone undergo mechanical amorphization which reduces crystallite size. The rate of amorphization of the milled zeolites was not accelerated by co-milling with the high-hardness oxides. However, the crystallite size of the milled samples has slightly decreased. The high-hardness corundum oxide initially becomes structurally distorted when they are co-milled with soft zeolite using a high-density milling medium. It is preferred to mill with high-

density powders as opposed to high-hardness oxides, which could cause greater amorphization and considerable microstructural changes in the raw zeolite. When the clinoptilolite is milled alone or in combination with other high hardness oxides, about 72-75% of the Cr(VI) can be removed from the water solution.

ACKNOWLEDGMENTS

This work has been supported by the Research office of the Mongolian National University of Education.

REFERENCES

1. Margeta K., Farkaš A. (2020) 'Introductory Chapter: Zeolites - from discovery to new applications on the global market'. Zeolites - New Challenges. 1-10. IntechOpen. https://doi.org/10.5772/intechopen.92907
2. Król M. (2020) Natural vs Synthetic zeolites. *Crystals*, **10**, 622. https://doi.org/10.3390/cryst10070622
3. *Behrman A.S., (1925) Early history of zeolites. Journal (American Water Works Association)*, **13**, 221-225. https://www.jstor.org/stable/41231725
4. Eroglu N., Emekci M., and Athanassiou C.G. (2017) Applications of natural zeolites on agriculture and food production. *J. Sci. Food Agriculture*, **97**, 3487-3499. https://doi.org/10.1002/jsfa.8312
5. Du G., Li Z., Liao L., Hanson R., Leick S., *et al*. (2012) Cr(VI) retention and transport through Fe(III)-coated natural zeolite. *J. Hazard. Mat.,* 221-222, 118-123. https://doi.org/10.1016/j.jhazmat.2012.04.016
6. Zeng Y., Woo H., Lee G., Park J. (2010) Adsorption of Cr(VI) on hexadecylpyridinium bromide (HDPB) modified natural zeolites. *Micropor. Mesopor. Mat.,* **130**, 83-91. https://doi.org/10.1016/j.micromeso.2009.10.016
7. Kosanović C., Bronić J., Subotić B., Smit I., Stubičar M., Tonejc A., Yamamoto T. (1993) Mechanochemistry of zeolites: Part 1. Amorphization of zeolites A and X and synthetic mordenite by ball milling. *Zeolites*, **13**, 261-268. https://doi.org/10.1016/0144-2449(93)90004-M
8. Kasai E., Mimura H., Sugiyama K., Saito F., Akiba K., Waseda Y. (1994) Mechano-chemical changes in natural and synthetic zeolites by dry grinding using a planetary ball mill. *Adv. Powder Technology,* **5**(2), 189-203. https://doi.org/10.1016/S0921-8831(08)60614-7

9. Majano G., Borchardt L., Mitchell S., Valtchev V., Pérez Ramírez J. (2014) Rediscovering zeolite mechanochemistry – A pathway beyond current synthesis and modification boundaries, *Micropor. Mesopor. Mat*., **194**, 106-114. https://doi.org/10.1016/j.micromeso.2014.04.006
10. Zolzaya T., Davaabal B., Ochirbat Z., Oyun-Erdene G., Minjigmaa A., Temuujin J. (2011) The mechanochemical activation study of Tsagaan-tsav zeolite. *Mong. J. Chem*., **12**, 98-10. https://doi.org/10.5564/mjc.v12i0.181
11. Bohacs K., Kristaly F., Mucsi G. (2018) The influence of mechanical activation on the nanostructure of zeolite. *J. Mater. Sci.,* **53**, 13779-13789. https://doi.org/10.1007/s10853-018-2502-2
12. Pabis-Mazgaj E., Gawenda T., Pichniarczyk P., Stempkowska A. (2021) Mineral composition and structural characterization of the clinoptilolite powders obtained from zeolite-rich tuffs. *Minerals,* **11**(10), 1030. https://doi.org/10.3390/min11101030
13. http://webmineral.com/data/Clinoptilolite-Na.shtml#.YflUTBf19Jk (last accessed January 10, 2022)
14. Adhi Putra I.M.W., Kusumawati I.G.A.W. (2018) The use of clinoptilolites as carrier of metformin hydrochloride in drug delivery system: *in vitro* drug release study. *Asian J. Pharm. Clin. Res.,* **11**(11), 285-289. https://doi.org/10.22159/ajpcr.2018.v11i11.24366
15. Mansouri N., Rikhtegar N., Panahi H.A., Atabi F., Shahraki B.K. (2013) Porosity, characterization and structural properties of natural zeolite – clinoptilolite – as a sorbent. *Env. Protec. Eng.,* **39**, 139-152. https://doi.org/10.5277/epe130111
16. Eskandari L., Kheiri F. (2018) Synthesis, characteristics and kinetic study of magnetic-zeolite nano composite for adsorption of zirconium. *Chem. Technol. Ind. J.*, **13**(3), 126.
17. Serna C.J., Rendon J.I., Iglesias J.E. (1982) Infrared surface modes in corundum-type microcrystalline oxides. *Spectrochim. Acta,* **38**A, 797-802. https://doi.org/10.1016/0584-8539(82)80070-6
18. Correcher V., Garcia-Guinea J., Bustillo M.A., Garcia R. (2009) Study of the thermoluminescence emission of a natural α-cristobalite. *Radiation Effects & Defects in Solids*, **164**, 59-67. https://doi.org/10.1080/10420150802270995